

On a fusion born triton effect in JET deuterium discharges with H-minority ion cyclotron range of frequencies heating

Original

On a fusion born triton effect in JET deuterium discharges with H-minority ion cyclotron range of frequencies heating / Kiptily, V. G.; Belli, F.; Eriksson, J.; Hellesen, C.; Goloborodko, V.; Schoepf, K.; Subba, F.. - In: NUCLEAR FUSION. - ISSN 0029-5515. - 59:6(2019). [10.1088/1741-4326/ab19f5]

Availability:

This version is available at: 11583/2986780 since: 2024-03-11T14:08:25Z

Publisher:

IOP PUBLISHING LTD

Published

DOI:10.1088/1741-4326/ab19f5

Terms of use:

This article is made available under terms and conditions as specified in the corresponding bibliographic description in the repository

Publisher copyright

IOP preprint/submitted version

This is the version of the article before peer review or editing, as submitted by an author to NUCLEAR FUSION. IOP Publishing Ltd is not responsible for any errors or omissions in this version of the manuscript or any version derived from it. The Version of Record is available online at <https://dx.doi.org/10.1088/1741-4326/ab19f5>.

(Article begins on next page)

Letter

On a fusion born triton effect in JET deuterium discharges with H-minority ICRF heating

V.G. Kiptily¹, F. Belli², J. Eriksson³, C. Hellesen³, V. Goloborod'ko⁴, K. Schöpf⁴ and JET contributors^a

¹ Culham Centre for Fusion Energy, UKAEA, Culham Science Centre, Abingdon, OX14 3DB, UK

² Unità Tecnica Fusione, ENEA C. R. Frascati, via E. Fermi 45, 00044 Frascati (Roma), Italy

³ Department of Physics and Astronomy, Uppsala University, SE-75120 Uppsala, Sweden

⁴ University of Innsbruck, Fusion@Österreichische Akademie der Wissenschaften (ÖAW), Innsbruck, Austria

^a See author list [X. Litaudon et al 2017 Nucl. Fusion 57 102001]

E-mail: vasili.kiptily@ukaea.uk

Received xxxxxx

Accepted for publication xxxxxx

Published xxxxxx

Abstract

An effect due to fusion born triton production has been observed in JET high-performance deuterium plasma discharges with NBI and H-minority ICRF heating, using DD and DT neutron spectrometry as well as fusion product loss measurements. The observations show that increase of the triton burn up rate leads to decrease of second harmonic $\omega = 2\omega_{cD}$ enhancement of the DD neutron rate and an acceleration of tritons due to absorbing ICRH power at the third harmonic $\omega = 3\omega_{cT}$. This effect indicates a redistribution of ICRH power absorption at $\omega \approx \omega_{cH} = 2\omega_{cD} = 3\omega_{cT}$ towards increase of triton concentration at the ion cyclotron resonance layer. It determines the necessity to consider the ICRH power absorption $\omega = 3\omega_{cT}$ in modelling of high-performance deuterium discharges with simultaneous NBI and H-minority ICRF heating for the development of DT plasma scenarios and fusion rate predictions.

Keywords: tokamak, fusion products, ICRF heating

In addition to the deuterium neutral beam injection (NBI), heating of deuterium plasmas with waves in the ion cyclotron range of frequencies (ICRF) is exploited to develop high-performance scenarios (H-mode, hybrid and advanced) in the preparation of forthcoming Joint European Torus (JET) deuterium tritium (DT) experiments [1]. In our case, in the hybrid scenario discharges with plasma current $I_p = 2.2$ MA and central toroidal field $B_T(0) = 2.8$ T, a combined deuterium NBI and hydrogen-minority ICRF heating $\omega \approx \omega_{cH} = 2\omega_{cD} = 3\omega_{cT}$ at $f = \omega/(2\pi) \approx 42.5$ MHz of dipole phasing is used. Applying ICRF heating (ICRH), power damping at $\omega = \omega_{cH}$ dominates, the neutron rate increases due to $\omega = 2\omega_{cD}$ damping by D-ions and the plasma performance is enhanced. As rule, ICRH power damping at $\omega = 3\omega_{cT}$ is neglected referring to a low tritium content. Here we will show that ignor the $\omega = 3\omega_{cT}$

damping by fusion born tritons is not resonable in high-performance discharges.

In the deuterium plasmas, neutrons are produced due to the fusion reaction $D + D = n$ (2.45 MeV) + ^3He (0.82 MeV). With roughly the same probability, the second branch of this fusion, $D + D = p$ (3.02 MeV) + t (1.01 MeV) gives rise to tritons. These tritons “burnup” during slowing down generates 14-MeV neutrons due to the reaction $D + T = ^4\text{He}$ (3.5 MeV) + n (14.1 MeV) with a maximum of the emission at resonance $E_T \approx 160$ keV in the cross-section. Previously, triton burnup measurements have been carried out on different tokamaks [2-7] studying confinement and slowing-down of fast tritons in deuterium plasmas. The DT neutron emission can reach up to

3% of the total neutron rate in JET high-performance deuterium discharges.

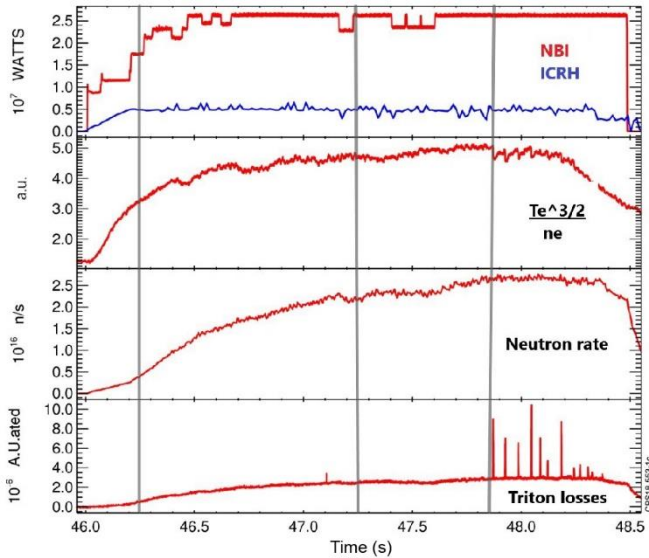


Figure 1. Waveforms of the discharge #92394 at $B_T(0)=2.8T$, $I_p=2.2MA$ with 26MW deuterium NBI and 5MW H-minority ICRH at $f=42.5MHz$. Grey vertical lines denote time slots: 46.25s – 47.25s is the low average triton burnup rate (LTB) and 47.25s – 47.85s is the high average triton burnup rate (HTB).

In this Letter we report on experimentally observed variations in DD and DT neutron spectra as well as fusion product losses which correlated with the rate of fusion born triton production in JET high-performance deuterium plasma discharges with NBI and H-minority ICRF heating.

Measuring neutrons by means of the time-of-flight spectrometer TOFOR [8] in the high-performance JET discharges, we observed some changes in DD neutron spectra, which are correlated with the increase of the triton burnup rate, i.e. 14-MeV neutron rate. We selected several similar hybrid discharges ##92393, 92394, 92395 and 92398, characterised by quiet and stable plasmas in two specific time periods, which were chosen for the analysis. As an example, waveforms of the discharge #92394 are shown in figure 1. We defined the time slot 46.25s – 47.25s as a period of low average triton burnup rate (LTB) and the time slot 47.25s – 47.85s as the period of high average triton burnup rate (HTB). In the LTB period the neutron rate is growing at a stable ICRH power. The slowing down parameter $\tau_e \sim T_e^{3/2}/n_e$ [9], where T_e and n_e are the electrons temperature and density, grows with some saturation at the end. Note, the triton burnup rate and the delay of 14-MeV neutron emission relative to total neutron rate depend on this parameter. Triton losses measured with the fast ion loss detector (FILD) [10] follow the neutron rate, which indicates a classical type of prompt fusion product loss. The HTB period is characterised by quite steady parameters with very small increase of neutron rate. This time slot was chosen in such a way as to avoid the unstable fishbone period of strong triton losses with typical spikes seen.

Figure 2 demonstrates why we selected these time slots as LTB and HTB rate periods. You can see waveforms of the total neutron rate together with relative 14-MeV neutron and 17-MeV γ -ray rates, which are associated with DT fusion. We used an NE213 detector based on a liquid scintillator with a tangential line-of-sight [11] for 14-MeV neutron measurements. This is a broadband neutron spectrometer of MeV energy-range, which allows recording DD and DT neutron spectra. Gamma-rays related to triton burnup are produced in the reaction $D + T = {}^5He + \gamma$ (16.84 MeV), which is a weak branch ($\sim 10^{-4}$) of the main DT fusion reaction giving rise to 14-MeV neutrons. These γ -rays were measured with bismuth-germanite detector (BGO), which is viewing the plasma in the tangential line-of-sight [12]. In the figure you can see that maximums of both 14-MeV neutrons and 17-MeV gammas are a bit shifted due to slowing down of tritons and increase of their density.

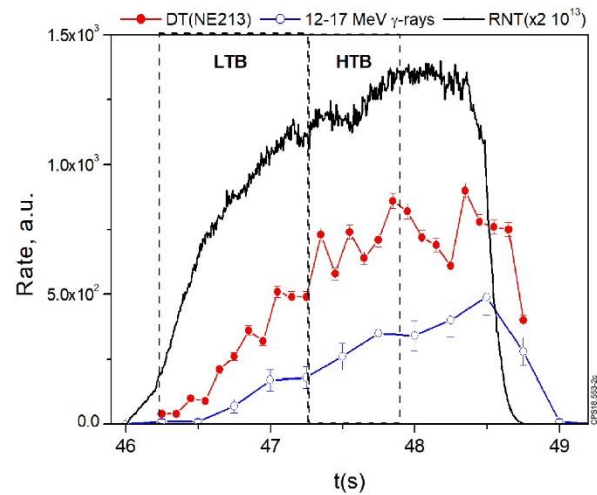


Figure 2. Waveforms of total neutron rate (solid line), DT-neutron rate detected with NE213 spectrometer (filled circles) and γ -ray rate in the energy window 12 -17 MeV detected with the bismuth-germanite (BGO) detector (open circles).

It was found that the TOFOR spectra recorded in LTB and HTB are rather different in all selected high-performance discharges. Indeed, in the discharge #92394 (figure 3), the number of neutrons detected with time of flight in the range $t_{TOF} = 45 - 55$ ns is much higher in the LTB period than in the HTB one. We need to note that the time of flight varies inversely with neutron velocity and energy: $t_{TOF} \sim \frac{1}{v_n} \sim \frac{1}{\sqrt{E_n}}$, and this t_{TOF} -range is related to DD neutron energies $E_n \approx 3.5 - 5.1$ MeV. The measured TOFOR spectra can be partitioned into components due to thermonuclear (TH), beam-thermal (NBI), ICRF heating induced (RF) and scattered neutrons [9, 13]. Such spectrum partitioning is displayed in figure 3 where the ICRH DD fusion neutrons in the LTB period are more energetic than those in the HTB period. This is also seen in figure 4 that presents the fitted

TOFOR neutron spectra as a function of the neutron energies E_n in the LTB and HTB rate periods.

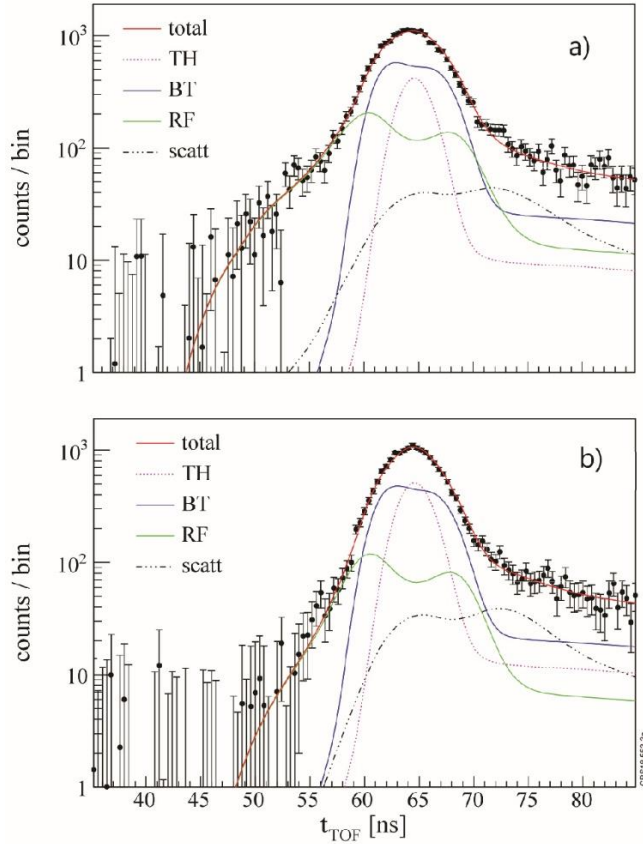


Figure 3. DD-neutron spectra recorded with the time-of-flight spectrometer TOFOR (dots): (a) spectrum recorded during the LTB rate period; (b) spectrum recorded during the HTB rate period. Lines are the fitted components of the spectra related to thermal (TH) and NBI beam – target neutrons (BT), neutrons due to ICRF D-ion acceleration at $\omega = 2\omega_{cD}$ (RF), backscattered neutrons (scatt).

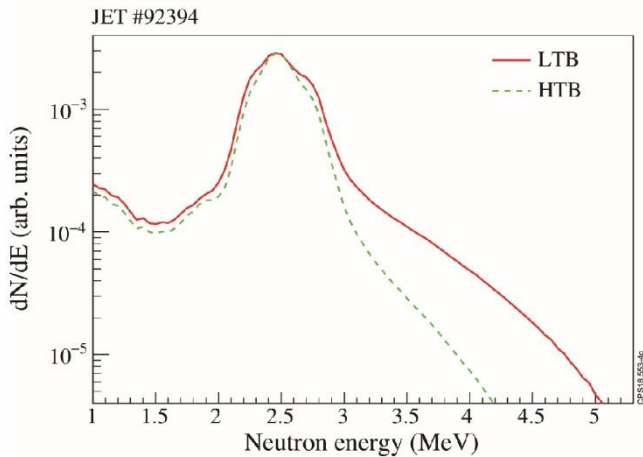


Figure 4. A comparison of neutron spectra fitted to the TOFOR data during the LTB and HTB rate periods.

According to kinematics of the $D(D, n)^3\text{He}$ reaction, the energy of neutrons depends on the energy of reacted

deuterons. In our case, the energy of ICRF accelerated deuterons is much higher than the bulk ion temperature, $E_D \gg T_D$, and $E_n = 2.45 \text{ MeV} + 0.5E_D + 0.5\sqrt{3E_D(3.27\text{MeV} + 0.5E_D)} \cos \theta_n$, where θ_n is an angle between neutron and deuteron velocities in the lab system. So, neutrons detected in the energy range $E_n \approx 3.5 - 5.1 \text{ MeV}$ were produced by deuterons energies $E_D \approx 0.25 - 1.35 \text{ MeV}$ (related to fully trapped deuterons and $\cos \theta_n \approx 1$ for TOFOR). Since the NBI deuterium energies were below 125 keV, such energetic neutrons appeared in the spectra due to ICRF acceleration of D-ions at $\omega \approx \omega_{cH} = 2\omega_{cD}$, and thus on average $\overline{E}_D^{LTB} > \overline{E}_D^{HTB}$.

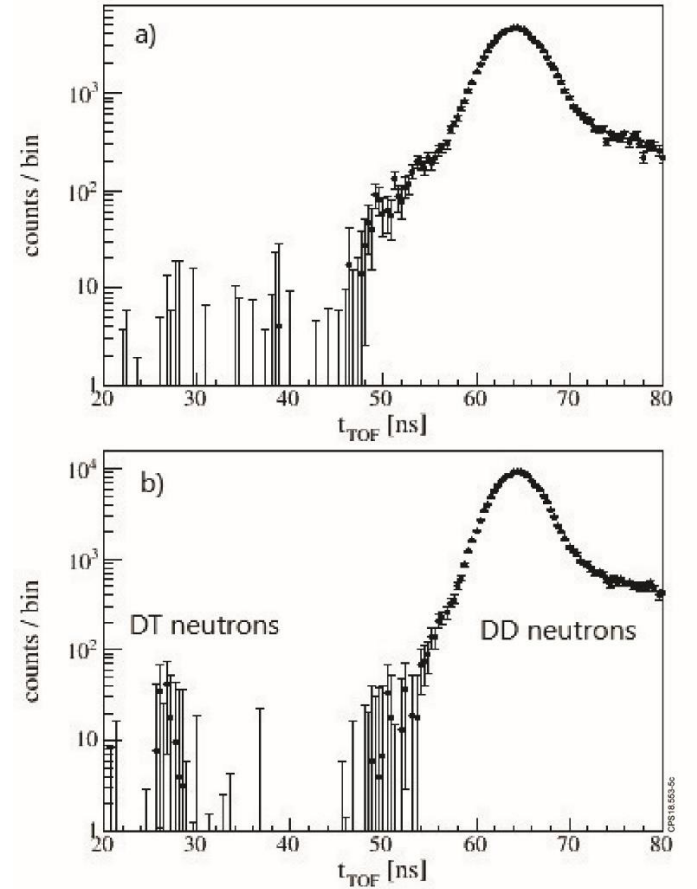


Figure 5. Sum of DD-neutron spectra recorded with time-of-flight spectrometer TOFOR in similar high-performance discharges ##92393, 92394, 92395 and 92398: (a) spectrum related to the LTB rate periods; (b) spectrum related to the HTB rate periods.

We observed the similar distinctive feature of TOFOR spectra in all selected discharges. The sums of the spectra in both chosen periods are presented in figure 5. It is important to note that in contrast to the spectrum in figure 5(a) referring to the LTB periods, a peak at $t_{TOF} \approx 27 \text{ ns}$ is evident in figure 5(b), which is related to 14-MeV neutrons due to triton burnup in the HTB period.

For analysis of the ICRH neutron enhancement we used the ratio $I_{RF}/(I_{TH} + I_{NBI})$ obtained from the least-square

fitting procedure of the spectrum components shown in figure 3. As an example, the ICRH neutron enhancement factors have been calculated and presented in figure 6 together with the waveforms of total neutron, DT neutron and 17-MeV γ -ray rates. One can see that during the HTB period this factor drops dramatically. Hence, this is an additional confirmation that the decrease of the second harmonic $\omega = 2\omega_{cD}$ deuteron acceleration results in the reduction of the intensity of energetic neutrons when the density of fusion born tritons increased.

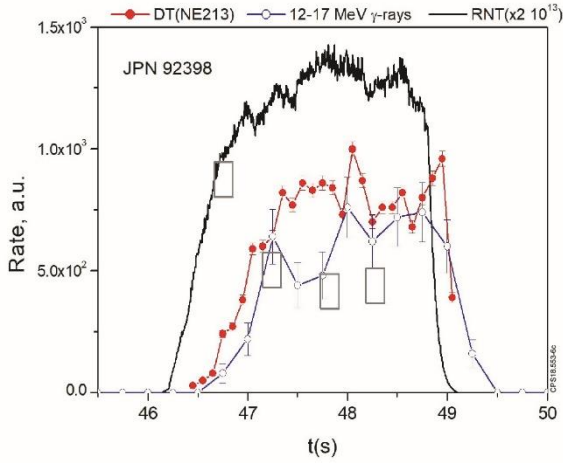


Figure 6. Waveforms of the high-performance discharge #92398 as shown in figure 3. Grey rectangulars denote the changes of the ICRH enhancement factor inferred from the TOFOR data.

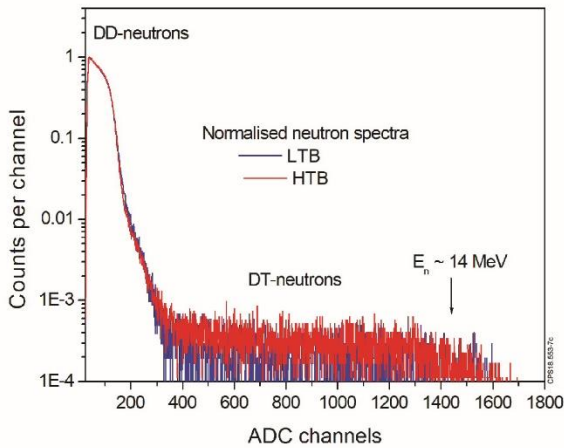


Figure 7. Sum of normalised neutron spectra recorded with NE213 spectrometer in similar high-performance discharges ## 92393, 92394, 92395 and 92398; blue - spectrum recorded during the LTB rate period; red – spectrum recorded during the HTB rate period.

Measurements with the NE213 detector allowed us to confirm the TOFOR results and to study the triton burnup directly, analysing both DD and DT neutron spectra. Neutron detection with the NE213 detector is based on elastic scattering of neutrons by light nuclei (ordinary hydrogen) in

the scintillator. This is a recoil/proton-recoil detector. Neutron transfers a portion of its kinetic energy E_n to a nucleus of mass A (recoil nucleus/proton) $E_R = \frac{4A}{(1+A)^2} E_n (\cos \theta_n)^2$. The recoil nucleus/proton loses its energy E_R in the scintillator. So, the recoil energies are distributed continuously between zero and the maximum possible, E_n in the case of mass $A = 1$; in our case it is related to $E_n^{DD} \approx 2.5$ MeV and $E_n^{DT} \approx 14.1$ MeV. The sum of normalised neutron spectra recorded with the NE213 spectrometer in the high-performance discharges ## 92393, 92394, 92395 and 92398, which are the same as those used for the TOFOR data analysis, is presented in figure 7. The summation was made in both LTB and HTB periods. An intensive DD peak and DT neutrons with a 14-MeV edge are clearly seen in the recoil spectra. A zoom of the high-energy tail of the DD part of the neutron recoil spectra is shown in figure 8. Hence the NE213 data confirm the TOFOR results, i.e. neutrons in LTB period are more energetic than in the HTB and thus $\bar{E}_D^{LTB} > \bar{E}_D^{HTB}$.

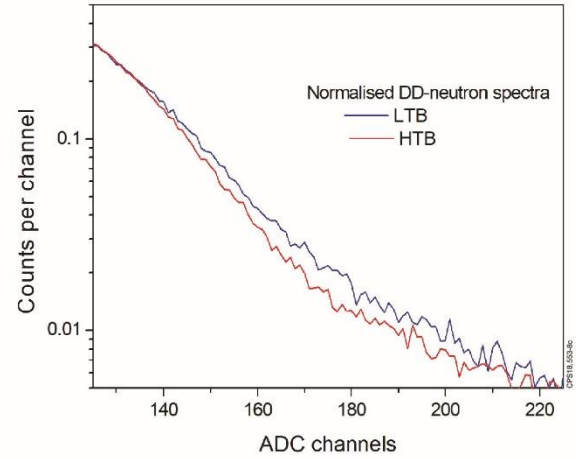


Figure 8. A part of the neutron spectra shown in figure 7, which is related to the high energy tail of DD-neutrons.

Neutron recoil spectra related to DT-neutrons are shown in figure 9. For the analysis of this low statistics data, we used a fitting of the logistic function $F(x) = \frac{A}{1+e^{k(x-x_0)}}$. Normalised fitted logistic curves related to the LTB and HTB rate periods are presented in figure 10(a). In the 1st approximation, the derivatives of the logistic function shown in figure 10(b) characterise neutron emission spectra due to triton burnup at the edge $E_n^{DT} \approx 14.1$ MeV. One can see that despite of a noisy DT neutron recoil spectra obtained in such a way carry some features, which are opposite to DD neutron spectra in the chosen time slots. Indeed, the HTB spectrum is broader (~10%) than the LTB one. Taking into account the kinematics of the reaction $T + D = {}^4\text{He}(3.5\text{MeV}) + n(14.1\text{MeV})$ in the case of $E_T \gg T_D$, which gives the dependence $E_n = 14.1 \text{ MeV} + 0.44E_T + 0.62\sqrt{E_T(17.6\text{MeV} + 0.4E_T)} \cos \theta_n$,

we conclude that tritons are - upon average - more energetic in the HTB period, $\overline{E}_T^{HTB} > \overline{E}_T^{LTB}$. Hence, this effect indicates an acceleration of tritons by absorbing ICRH power at $\omega = 3\omega_{cT}$ due to a redistribution of ICRH power absorption associated with the increase of triton concentration at the ion cyclotron resonance layer.

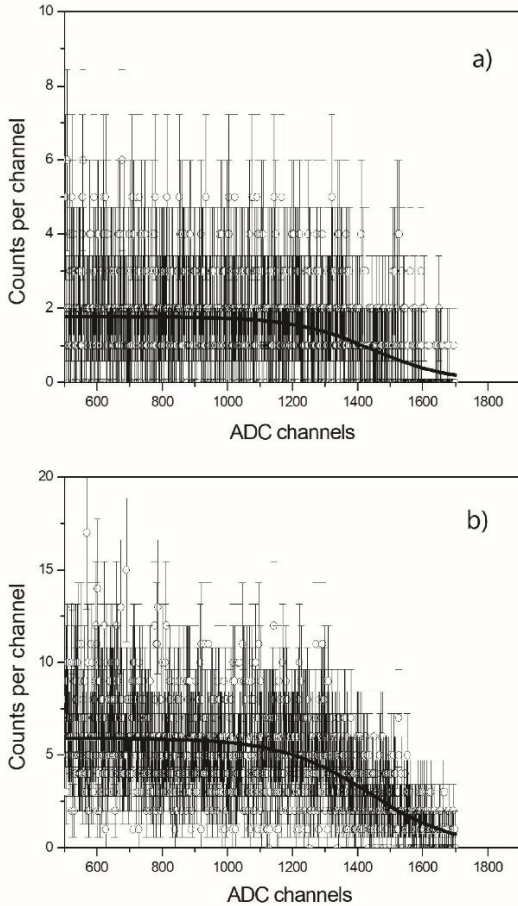


Figure 9. A part of the neutron spectra shown in figure 7, which is related to DT-neutrons: (a) spectrum related to the LTB rate period; (b) spectrum related to the HTB rate period; solid line – a fitted logistic curve (see text).

A correlation with triton production was also observed by FILD measured fusion product losses. A typical footprint of the losses recorded in discharge #92394 is presented in figure 11. Striking the scintillator plate, both lost fusion tritons (≈ 1 MeV) and protons (≈ 3 MeV) induce light collected with the CCD camera. However, light emission produced by tritons dominate ($\sim 90\%$) because protons are too energetic to stop in the thin scintillator layer entirely.

We compared the gyro-radius distributions of lost tritons in both LTB and HTB periods integrating the highest light output (dash line in figure 11) in the pitch-angle range $55^\circ - 58^\circ$, which is relevant to the FILD instrumental width. The smoothed and normalised gyro-radius distributions in figure

12(a) show that light emission recorded in the HTB rate period is shifted to higher gyro-radii relative to the LTB one. In this discharge the triton energy is related to the gyro-radius as $E_T(\text{MeV}) \approx 0.1 + 0.0075 \rho(\text{cm})^2$, so the lost triton energy distributions depicted in figure 12(b). It becomes evident that tritons lost in the period of the HTB rate are more energetic, thus FILD data confirm the results of the DT neutron measurements with the NE213-detector, i.e. $\overline{E}_T^{HTB} > \overline{E}_T^{LTB}$.

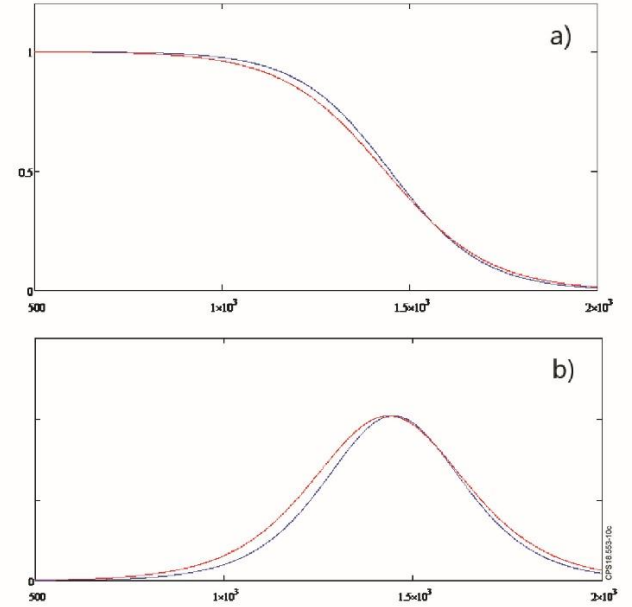


Figure 10. Normalised logistic curves (a) shown in figure 9 and their derivatives (b) related to the LTB (blue) and HTB (red) rate periods.

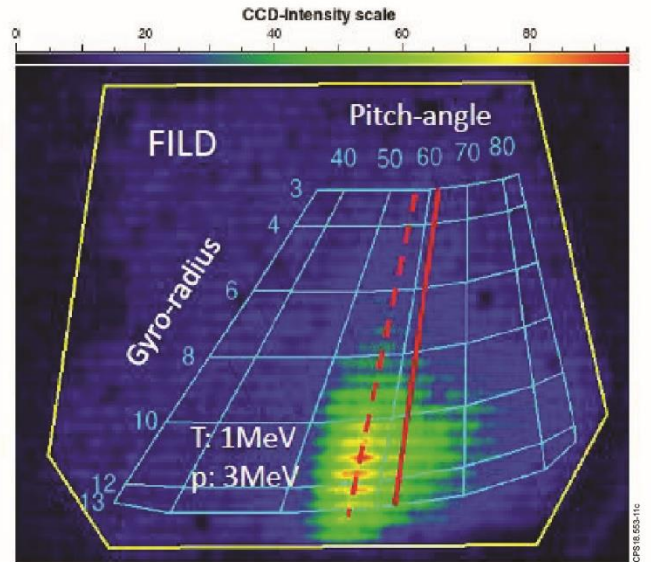


Figure 11. A footprint of ion losses in discharge #92394 obtained with FILD: red solid line – position of the IC resonance on the gyro-radius vs pitch-angle grid; dash red line – pitch-angle related to maximum light emission produced by lost fusion tritons and protons.

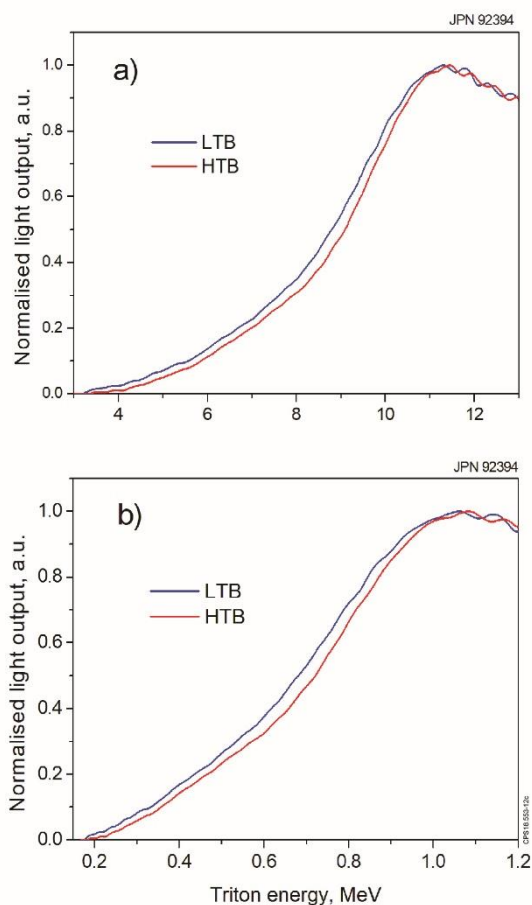


Figure 12. Smoothed gyro-radius (a) and energy (b) distributions of lost tritons related to the maximal FILD light emission (dash line in figure 11); the distributions are averaged over the pitch-angle instrumental width $\sim 55^\circ - 58^\circ$.

Summarising the results obtained in the selected high-performance discharges with NBI and H-minority ICRF heating, we ascertain the following:

- DD neutron measurements with TOFOR show that the average deuteron energies $\bar{E}_D^{LTB} > \bar{E}_D^{HTB}$.
- The ICRF neutron enhancement factor due to $\omega = 2\omega_{cD}$ is decreasing in the HTB rate period due to the increase of the triton burnup rate and the growing triton density in vicinity of the ion cyclotron resonance layer. However, we leave room for other effects which could impact on the neutron enhancement.
- DD neutron measurements with the NE213-detector confirm the TOFOR data.
- DT neutron measurements with the NE213-detector show that the spectrum related to the HTB rate period is broader than the spectrum related to the LTB one, and that the average triton energies $\bar{E}_T^{HTB} > \bar{E}_T^{LTB}$. A balance between slowing down and acceleration of tritons due to $\omega \approx \omega_{cH} = 2\omega_{cD} = 3\omega_{cT}$

ICRF power absorption is the only plausible explanation of this effect.

- Gyro-radius/energy distributions of lost tritons measured with FILD are consistent with DT neutron measurements indicating that the average triton energies $\bar{E}_T^{HTB} > \bar{E}_T^{LTB}$.

In conclusion, the presented effects demonstrate evident redistribution of ICRF power absorption at $\omega \approx \omega_{cH} = 2\omega_{cD} = 3\omega_{cT}$ and an acceleration of tritons due to absorbing ICRF power at $\omega = 3\omega_{cT}$ as the triton concentration at the IC resonance layer increases. Hence, developing high performance deuterium plasma scenarios with NBI and H-minority ICRF heating for application in DT experiments, the 3rd harmonic triton damping of ICRH should be considered. Further we note that triton burnup measurements in high performance deuterium plasma discharges can help in validation of auxiliary ICRF plasma heating models and optimisation of plasma scenarios.

Acknowledgements

We are grateful to C. Challis, S. Sharapov, K. McClements, H. Weisen, Ye. Kazakov, D. Van Eester and M. Mantsinen for fruitful discussions. This work has been carried out within the framework of the EUROfusion Consortium and has received funding from the Euratom research and training programme 2014-2018 under grant agreement No 633053 and from the RCUK Energy Programme [grant No EP/P012450/1]. To obtain further information on the data and models underlying this paper please contact PublicationsManager@ukaea.uk. The views and opinions expressed herein do not necessarily reflect those of the European Commission.

References

- [1] Litaudon X. *et al* 2017 *Nucl. Fusion* **57** 102001
- [2] Heidbrink W. W., Chrien R.E. and Strachan J. D., 1983 *Nucl. Fusion* **23** 917
- [3] Källne J. *et al* 1988 *Nucl. Fusion* **28** 1291
- [4] Conroy S. *et al* 1988 *Nucl. Fusion* **28** 2127
- [5] Strachan J.D. *et al* 1996 *Nucl. Fusion* **36** 1189
- [6] Nishitani T. *et al* 1996 *Plasma Phys. Control. Fusion* **38** 355
- [7] Ballabio L. *et al* 2000 *Nucl. Fusion* **40** 21
- [8] Stitzer L. Jr, *Physics of Fully Ionized Gases*, Interscience, New York (1962)
- [9] Gatun Johnson M. *et al* 2008 *Nucl. Instrum. Methods Phys. Res.* **A591** 417
- [10] Darrow D. *et al* 2006 *Rev. Sci. Instrum.* **77** 10E701
- [11] Belli F. *et al* 2012 *IEEE Trans. Nucl. Science* **59** 2512-19
- [12] Kiptily V. *et al* 2002 *Nucl. Fusion* **22** 999-1007
- [13] Hellesen C. *et al* 2010 *Nucl. Fusion* **50** 022001